

Efficient removal of Pb (II) and Cd (II) from water by cross-linked poly (N-vinylpyrrolidone-co-maleic anhydride)@eggshell/Fe₃O₄ environmentally friendly nano composite

Ehsan Nazarzadeh Zare^{a,*}, Moslem Mansour Lakouraj^b, Mahsa Masoumi^b

^aSchool of Chemistry, Damghan University, Damghan, P.O. Box 36716-41167, Iran, Tel. +982335220095, Fax +982335220095, email: ehsan.nazarzadehzare@gmail.com, e.nazarzadeh@du.ac.ir (E.N. Zare)

^bPolymer Research Laboratory, Department of Organic Chemistry, Faculty of Chemistry, University of Mazandaran, Babolsar, P.O. Box 47416-95447, Iran, Tel. +981125342383, Fax +981125342383, email: lakouraj@umz.ac.ir (M.M. Lakouraj), masumi.mahsa68@gmail.com (M. Masoumi)

Received 17 November 2019; Accepted 23 February 2018

ABSTRACT

A novel environmentally friendly super-paramagnetic nano composite based on cross-linked poly (N-vinylpyrrolidone-co-maleic anhydride) (PNVPMA) was successfully prepared by simultaneous reaction of the PNVPMA copolymer with 3-aminobenzoic acid (3ABA), as a modifying agent, and ethylenediamine, as a cross linking agent, in the presence of Fe₃O₄ nano particles and eggshell. The prepared materials were characterized by Fourier transform infrared spectroscopy (FT-IR), X-ray diffraction (XRD), scanning electron microscopy (SEM) and atomic force microscopy (AFM). Vibrating sample magnetometer (VSM) was used to measure the magnetic property of nano composite as a function of magnetic field. The uptakes of Pb (II) and Cd (II) on the nano composite were studied in a batch system. The influences of various factors including pH of solution, nano composite dosage, agitation time, and initial concentrations of Pb (II) and Cd (II) were also investigated. The maximum adsorption capacities (Q_{max}) of Pb (II) and Cd (II) on the nano composite under the certain experimental conditions were 312.5 mg/g and 32.78 mg/g, respectively. The results showed that the experimental data of the Pb (II) and Cd (II) adsorption on the nano composite were in agreement with the Langmuir adsorption isotherm and second-order kinetic equations. The negative values of ΔG° for the adsorption of both Pb (II) and Cd (II) on the synthesized nano composite endorse that the adsorption processes are spontaneous and thermodynamically favorable. On the other hand, the positive values of ΔH° support the endothermic physical adsorption process.

Keywords: Poly (N-vinylpyrrolidone-co-maleic anhydride); Nano composite; Pb (II) and Cd (II) removal; Environmentally friendly

1. Introduction

Currently, the heavy metal ions contamination of wastewater is the most important environmental problem throughout the world due to the mobility of these contaminants in natural water ecosystems and their toxicity [1]. Heavy metals are commonly known as those metals which have high atomic weights and a specific density greater

than 5.0 [1,2]. Dissolved heavy metals ions into the water are dangerous for the environment and humans and their accumulation in the food chain can cause serious diseases [3]. Heavy metal ions poisoning depends on several factors including the quantity, method of contact, chemical nature and nutritional status of exposed persons [2,3]. The diseases, such as high blood pressure, kidney damage, destruction of testicular tissue, osteoporosis and destruction of red blood cells are examples of poisoning caused by Pb (II) and Cd (II) heavy metals [1,4].

*Corresponding author.

Many papers reported the removal of metallic ions from water by using by the different adsorbents [5–11]. Up to now, many techniques such as ion exchange, precipitation, adsorption, and membrane process have been represented to remove heavy metal ions from water [12]. Among them, adsorption is a simple and in expensive technique for there move of heavy metal ions contaminations [13–17].

Synthesized copolymers of reactive or functional monomers are steadily achieving importance. Many copolymers with reactive functional groups are now being synthesized [17–22]. These functional groups provide an approach to a subsequent modification of the polymer for the specific end applications [17–22]. Poly (N-vinylpyrrolidone-co-maleic anhydride) (PNVPMA) is a good biocompatible copolymer due to its hydrophilic nature and low toxicity [22]. Also, PNVPMA copolymer has reactive groups in the main chain structure for further functionalization.

On the other hand, the use of the low-cost waste materials for the achievement of the eco-friendly composite adsorbent is promising for researchers [23–27]. Among waste materials, eggshell is economically cheap, plentiful in nature and has intrinsic pore structure. Eggshell contains calcium carbonate (94%), magnesium carbonate (1%), calcium phosphate (1%), and organic matter (4%) [21]. A few researchers reported the composites based on eggshell for water treatment [26–28]. The magnetic nano particles are used to facilitate the separation process. Many researchers have been reported the use of polymer based magnetic nano composites for the removal of heavy metal ions [13–17,29–32].

No studies on the synthesis, characterization and use of the CPNVPMA@eggshell/Fe₃O₄ environmentally friendly nano composite as an adsorbent for the removal of Pb (II) and Cd (II) from aqueous solution have been reported to date. The final goal of the current work is the development of a low cost, eco-friendly, functionalized, metal coordinated material based on cross-linked poly (N-vinylpyrrolidone-co-maleic anhydride), eggshell and iron oxide as an effective adsorbent for the Pb (II) and Cd (II) removal. The synthesized materials were characterized using the Fourier transform infrared (FTIR) spectroscopy, proton nuclear magnetic resonance (¹H-NMR) spectroscopy, X-ray diffraction (XRD), scanning electron microscopy (SEM), atomic-force microscopy (AFM) and vibrating sample magnetometer (VSM). The adsorption studies on the synthesized nano composite were carried out under different conditions, including agitation time, pH of solution, nano composite dosages and initial metal ions concentrations. Furthermore, the kinetic and thermodynamic studies of the adsorption data were examined.

2. Experimental

2.1. Materials

N-vinyl-2-pyrrolidone (NVP) (Sigma-Aldrich) was purified before use by distillation under moderate vacuum. All solvents, maleic anhydride (MA), benzoyl peroxide (BPO), 3-aminobenzoic acid (3ABA), ammonium hydroxide, ethylenediamine (EDA), FeCl₃·6H₂O, FeCl₂·4H₂O, Pb(NO₃)₂, Cd(NO₃)₂ and other inorganic chemicals including HCl and

NaOH were purchased from Merck Company and used without further purification.

2.2. Characterization techniques

FTIR spectra of the synthesized materials were carried out using Bruker Tensor 27 spectrometer (Bruker, Karlsruhe, Germany) in 400–4000 cm⁻¹ region using KBr pellets. ¹H-NMR spectrum was taken in DMSO-d₆ on a Bruker Avance DRX 400 MHz spectrometer (Germany), using tetramethylsilane as an internal reference. The surface morphology of the synthesized materials imaged by SEM (Hitachi S4160 instrument) and AFM (Nano surf easy Scan flex AFM (made of Switzerland)) measurements. The XRD patterns of the synthesized materials were recorded on an X'pert Philips X-ray photo electron spectrometer (The Netherlands) with non-monochromated Mg K α radiation as the excitation source. Magnetization measurement was performed by using a VSM Meghnatis Daghigh Kavir Corporation (Kashan, Iran). APHS-3C pH-meter (Shanghai, Tianyou) was applied for pH measurements. The metal ions concentration in the aqueous solution was measured by use of a flame atomic absorption spectrophotometer (AAS) (Hewlett-Packard 3510).

2.3. Synthesis of poly (N-vinylpyrrolidone-co-maleic anhydride) (PNVPMA)

The poly (N-vinylpyrrolidone-co-maleic anhydride) (PNVPMA) copolymer was synthesized using NVP and MA by radical initiated copolymerization. Briefly, equimolar amounts of NVP (1.1 mL) and MA (0.98 g) were combined in a 100 mL round bottom flask with BPO and 1,4-dioxane. The mixture was degassed by nitrogen to remove oxygen from the reaction vessel prior to copolymerization. Copolymerization reaction was carried out for 24 h at 94°C under nitrogen atmosphere. The copolymerization product was diluted in 1,4-dioxane followed by drop wise addition into a 100-fold excess (v/v) of diethyl ether in order to precipitate pure PNVPMA copolymer, which was then filtered and dried under vacuum at room temperature.

FT-IR (KBr): 3300–3450 cm⁻¹ (OH related to entrapped hydrate), 2800–2980 cm⁻¹ (aliphatic CH), 1852 cm⁻¹ (C=O anhydride), 1782 cm⁻¹ (C=O anhydride), 1725 cm⁻¹ (C=O NVP), range of 649–739 cm⁻¹ C-(CH₂)-C of parent chain [22].

¹H-NMR (400 MHz, DMSO): Δ 4.8, Δ 4.0 and Δ 3.5 ppm (ring methyl protons in NVP resonate), Δ 3.5–2.5 ppm (CH₂ main chain backbone resonates), Δ 6.2 ppm (protons of maleic anhydride resonate [22]).

2.4. Synthesis of cross-linked poly (N-vinylpyrrolidone-co-maleic anhydride) (CPNVPMA)

The cross-linked PNVPMA copolymer was prepared through a simultaneous reaction using the PNVPMA copolymer, 3ABA, as a modifying agent, and EDA, as a cross linking agent. The molar ratios of PNVPMA, 3ABA and EDAwere 1, 0.5, and 0.25, respectively. The reaction mixture was stirred at reflux for 5 h under inert gas. The obtained product (CPNVPMA) filtered, washed thoroughly with DMF and dried in a vacuum oven at 80°C for 24 h.

FT-IR(KBr): 3200–3430 cm^{-1} (acidic OH + NH amide), 3029–3061 cm^{-1} (aromatic CH), 2880–2980 cm^{-1} (aliphatic CH), 1705 cm^{-1} (C=O acid), 1663 cm^{-1} (C=O amide), 1431 cm^{-1} (C=C substituted benzene), 1286 cm^{-1} (C–N–H), 1103 cm^{-1} (C–N).

2.5. Preparation of eggshell nano particles

For the preparation of eggshell nano particles, firstly 5 g eggshell was milled by mortar to obtain a homogeneous free flowing powder. Then, the obtained eggshell powder washed three times with deionized water and acetone and then dried at 50°C for 5 h. Afterward, eggshell powder was placed in a round-bottomed flask equipped with inlet and outlet of N_2 under sonication bath with agitation 53 KHz at room temperature for 2 h. The particle size of the eggshell was approximately 45 nm.

FT-IR (KBr): 405 (lattice vibrations of CaO) and 1424, 875, and 710 cm^{-1} are associated with the asymmetric stretch, out of plane bend and in-plane bend vibration modes for CaCO_3 molecules [31].

2.6. Synthesis of Fe_3O_4 nano particles

The Fe_3O_4 nano particles were synthesized via a co-precipitation route according to our previous work [32]. The particle size of the Fe_3O_4 nano particles was approximately 50 nm.

FT-IR (KBr): 3369 cm^{-1} (–OH), 670 cm^{-1} (Fe–O–Fe)[32].

2.7. Preparation of CPNVPMA@ eggshell/ Fe_3O_4 environmentally friendly nano composite

The CPNVPMA@ eggshell/ Fe_3O_4 nano composite in optimum ratio was prepared via simultaneous reaction using the PNVPMA copolymer, 3ABA, as a modifying agent, and EDA, as a cross linking agent in the presence of Fe_3O_4 (0.5 g) and eggshell (0.5 g). The molar ratios of PNVPMA, 3ABA and EDA were 1, 0.5, and 0.25, respectively. The reaction mixture was stirred at reflux for 5 h under inert gas. The achieved CPNVPMA@ eggshell/ Fe_3O_4 nano composite filtered, washed thoroughly with DMF and dried in a vacuum oven at 80°C for 24 h.

2.8. Adsorption studies

The CPNVPMA@ eggshell/ Fe_3O_4 nano composite was employed as an adsorbent for the removal of Pb (II) and Cd (II) ions from aqueous solutions. Adsorption experiments were carried out through a batch route [13]. The adsorption equilibrium experiments consist the effect of solution pH values (2.0–8.0), composite nano adsorbent dosage (12–200 mg), initial ions concentration of Pb(II) and Cd(II) (30–400 mg L^{-1}) and the agitation time (20–40 min) on adsorption, designation of the maximum binding capacity, isotherm, kinetics and thermodynamic of adsorption. The influence of each factor was investigated under constant conditions of 50 mg of adsorbent powder, dispersed in 50 mL of Pb (II) and Cd (II) solutions (50 mg L^{-1}), for 180 min with stirring (300 rpm) at the temperature 298 K, while changing the initial level of the studied factor. After the equilibrium reached in all the

experiments, the two phases were separated and the concentration of ions (Pb (II) and Cd (II)) studied using AAS. The adsorption percentage of ions (Pb (II) and Cd (II)) (S%) was measurement using the following equation [15]:

$$S\% = \left(\frac{C_i - C_e}{C_i} \right) \times 100 \quad (1)$$

where C_i and C_e are the initial and final concentration of Pb (II) and Cd (II) ions in the solution (mg/L) before and after sorption, respectively.

2.9. Adsorbent regeneration and reuse

Adsorption–desorption equilibrium at three consecutive cycles were done to investigate the regeneration of the nano composite. Adsorption process was applied in a batch experiment for 3 h. Then, the nano composite was magnetically separated from the solution and then washed moderately with deionized water to remove the followed solution. The collected nano composite was then dispersed into 50 mL of 0.1 M HCl and shaken at 300 rpm shortly for 1 h to regenerate the nano composite adsorbent. The desorption percentage (D%) was measured as follows [16]:

$$\%D = \frac{A}{B} \times 100 \quad (2)$$

where A and B are the metal ions amount desorbed to the elution medium (mg) and the metal ions amount adsorbed on the adsorbent (mg).

3. Results and discussion

Nowadays, pollution of drinking water with heavy metals ions such as Pb (II) and Cd (II) is harmful for humans and animals, due to the fact that they are not biodegradable and aggregate in body tissues. On the other hand, due to lack of clean drinking water on the earth's surface, removal of heavy metals ions contaminations from water is a vital problem. In the present research, we describe a novel environmentally friendly super-paramagnetic nano composite based on CPNVPMA as an effective adsorbent for the Pb (II) and Cd (II) removal from aqueous solutions. Fig. 1 demonstrates the schematic construction method used to prepare the CPNVPMA@ eggshell/ Fe_3O_4 nano composite.

3.1. Characterization of the adsorbent

Fig. 2 demonstrates the FT-IR spectra of PNVPMA, CPNVPMA and CPNVPMA@eggshell/ Fe_3O_4 nano composite. In FTIR spectrum of CPNVPMA@egg shell/ Fe_3O_4 nano composite, the peaks in the ranges 3200–3405, 3000–3150, 2800–2950, 1550–1670, 1417, 850 and 500–580 cm^{-1} were assigned to the stretching vibrations of acidic hydroxyl and amide N-H, aromatic C-H, aliphatic C-H, acidic and amide carbonyls, C=C benzene ring, CaCO_3 molecules and Fe–O–Fe, respectively. According to the FTIR characteristic peaks of raw materials and compared to FTIR spectrum of nano composite, it can be concluded that the CPNVPMA@egg-shell/ Fe_3O_4 nano composite was successfully fabricated.

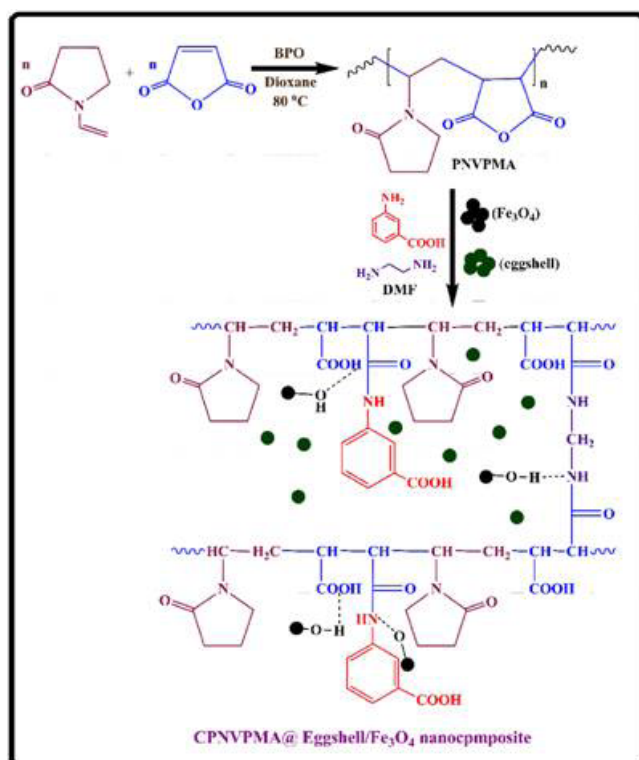


Fig. 1. Schematic pathway for construction of CPNVPMMA@eggshell/ Fe_3O_4 nano composite.

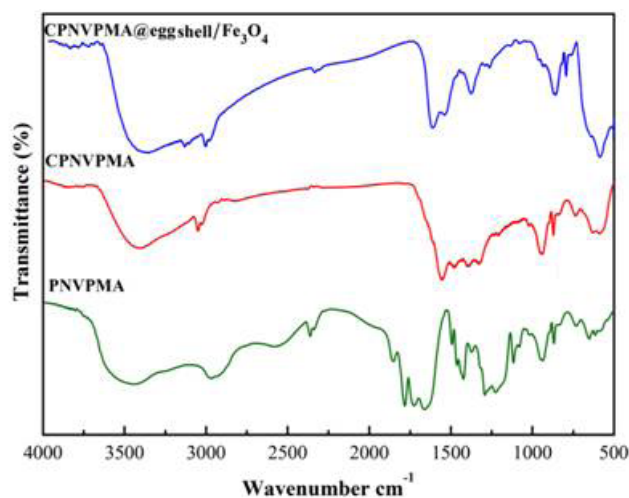


Fig. 2. FTIR spectra of PNVPMMA, CPNVPMMA, and CPNVPMMA@eggshell/ Fe_3O_4 nano composite.

Fig. 3 shows the XRD patterns of CPNVPMMA, eggshell and CPNVPMMA@eggshell/ Fe_3O_4 nanocomposite. The XRD pattern of CPNVPMMA showed amorphous nature with one peak at $2\theta = 20^\circ$ while XRD pattern of eggshell displayed numerous peaks at $2\theta = 22^\circ, 30^\circ, 36^\circ, 39^\circ, 43^\circ, 48^\circ, 50^\circ, 58^\circ$ and 64° corresponding to calcium carbonate [33]. The XRD pattern of Fe_3O_4 (not shown) exhibited a highly ordered stacked structure [32]. The XRD pattern of CPNVPMMA@eggshell/ Fe_3O_4 nano composite revealed a nearly crystal-

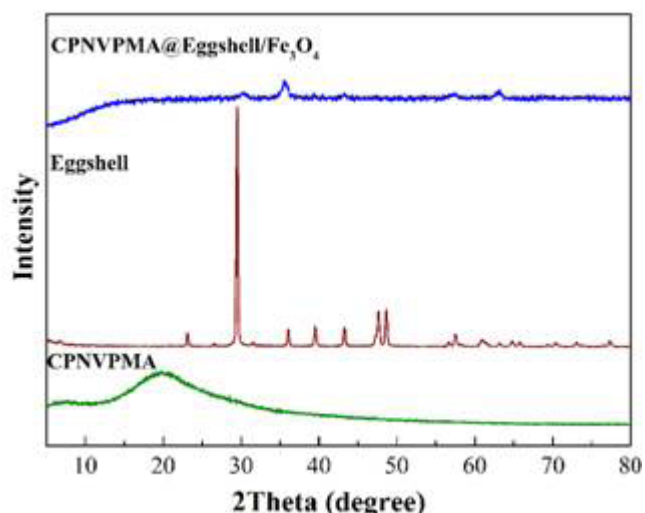


Fig. 3. XRD patterns of the CPNVPMMA, eggshell and CPNVPMMA@eggshell/ Fe_3O_4 nano composite.

line structure. The representative peaks associated to the eggshell, Fe_3O_4 nano particles and CPNVPMMA copolymer were distinguished in the XRD pattern of the CPNVPMMA@eggshell/ Fe_3O_4 nanocomposite. By comparing the results of FTIR spectroscopy and XRD patterns, we can conclude that CPNVPMMA@eggshell/ Fe_3O_4 nano composite was successfully prepared.

SEM was used to describe the morphology of the CPNVPMMA, eggshell and CPNVPMMA@eggshell/ Fe_3O_4 nano composite (Fig. 4). As can be seen in Fig. 4a, the CPNVPMMA has irregular morphology with an average diameter of 50 nm, while in the SEM image of eggshell (Fig. 4b) the particles aggregate together into small bulk on the surface with an average diameter of 45 nm. The SEM image of CPNVPMMA@eggshell/ Fe_3O_4 nanocomposite (Fig. 4c) shows well-defined spherical cluster nano structures with the average diameter of 55 nm. To the best of our knowledge, although cluster structures have smaller surface area than other structures, they have higher activity toward adsorption of metal ions [34]. This may be due to unique structure of cluster shape, consisting of aggregated spheres, and porosity of porous nanosheets [34].

AFM was used to observe the morphological properties including surface porosity, roughness and texture, micro graphs of the surface and cross-section of the CPNVPMMA@eggshell/ Fe_3O_4 nanocomposite. Fig. 5 displays the typical 2-dimensional (2-D) and 3-dimensional (3-D) AFM images of the CPNVPMMA@eggshell/ Fe_3O_4 nanocomposite. It is clear in both cases that the surface of the nano composite is homogenous, more uniform, smooth and compact without any cracks or pinholes.

Fig. 6 demonstrates the magnetization measurements for the CPNVPMMA@eggshell/ Fe_3O_4 nanocomposite. From Fig. 6 it can be seen that the nano composite displays a clearly hysteretic behavior with the value of saturation magnetization M_s : 15 emu/g. The hysteresis loop reveals a soft super-paramagnetic behavior, indicating that the nano composite can be controlled by external magnetic fields. The magnetic separability of the nano composite was verified by employing a magnet near the glass bottle (Fig. 6, inset).

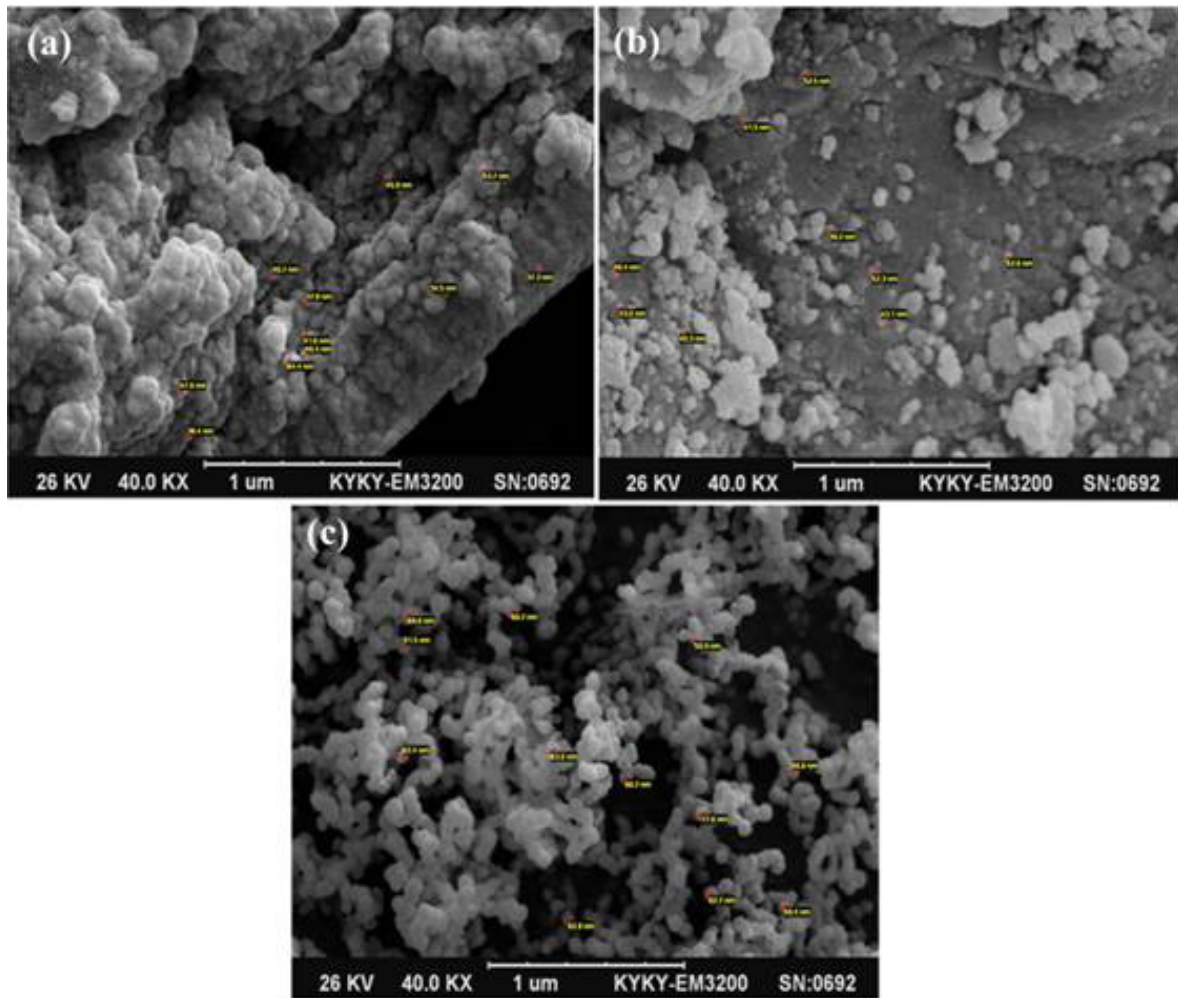


Fig. 4. SEM micro graphs of CPNVPMA (a), eggshell (b) and CPNVPMA@eggshell/Fe₃O₄ nano composite (c).

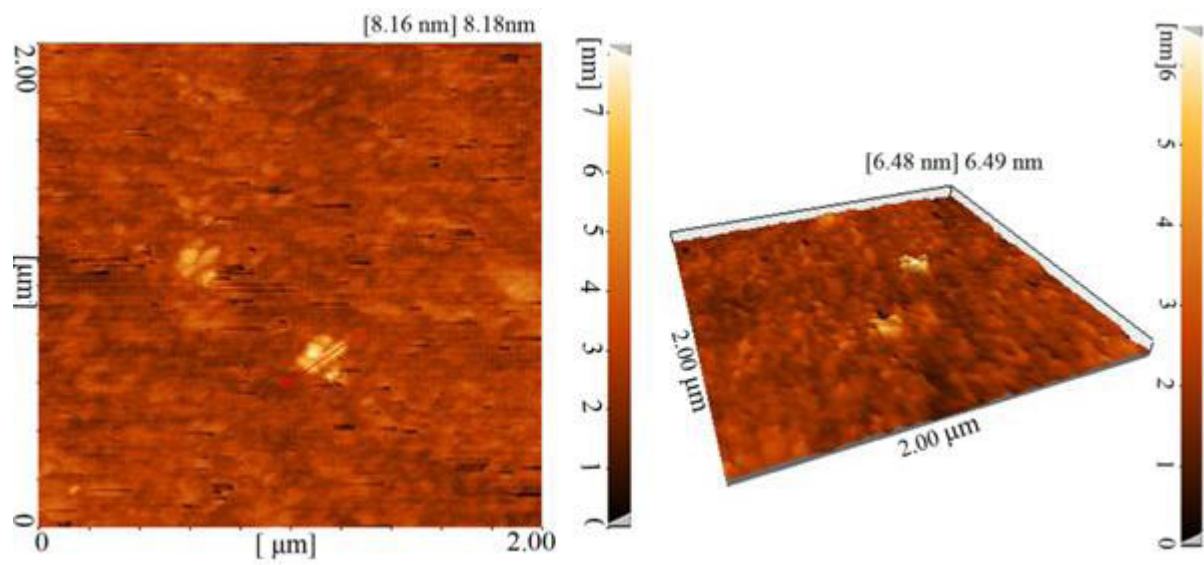


Fig. 5. AFM images of CPNVPMA@eggshell/Fe₃O₄ nano composite.

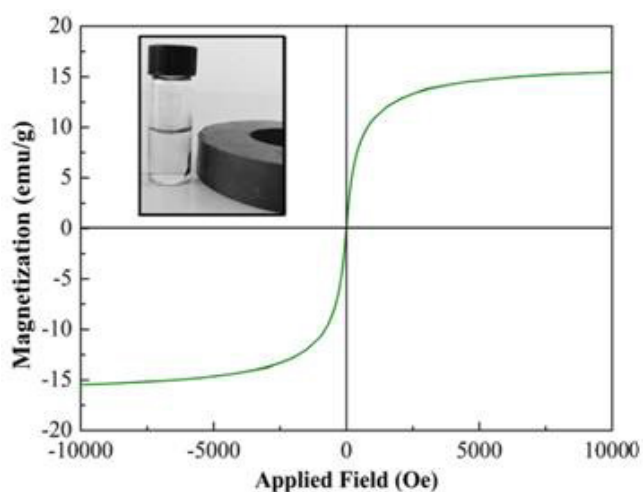


Fig. 6. VSM of CPNVPMA@eggshell/ Fe_3O_4 nano composite.

It was seen that the nano composite is attracted toward the magnet in a short period.

3.2. Adsorption studies

3.2.1. Effect of pH

The pH of the aqueous solution affects the charge on the surface of the adsorbents, thus it is a significant factor affecting the adsorption of heavy metal ions. Adsorption experiments were carried out at six different initial pH values (pH = 2–8).

As can be seen in Fig. 7a, the maximum percentage removal of Pb (II) and Cd (II) ions on the nano composite particles was at pH = 6 (Pb (II) (93.4%) and Cd (II) (90.5%)). On the other hand, at high pH = 8 the concentration of H^+ decreases and more surface functional groups are deprotonated to provide available sorption sites for Pb (II) and Cd (II), leading to an increase in the sorption percentage. In fact, the existence of amide and carboxyl groups on the cross-linked copolymer

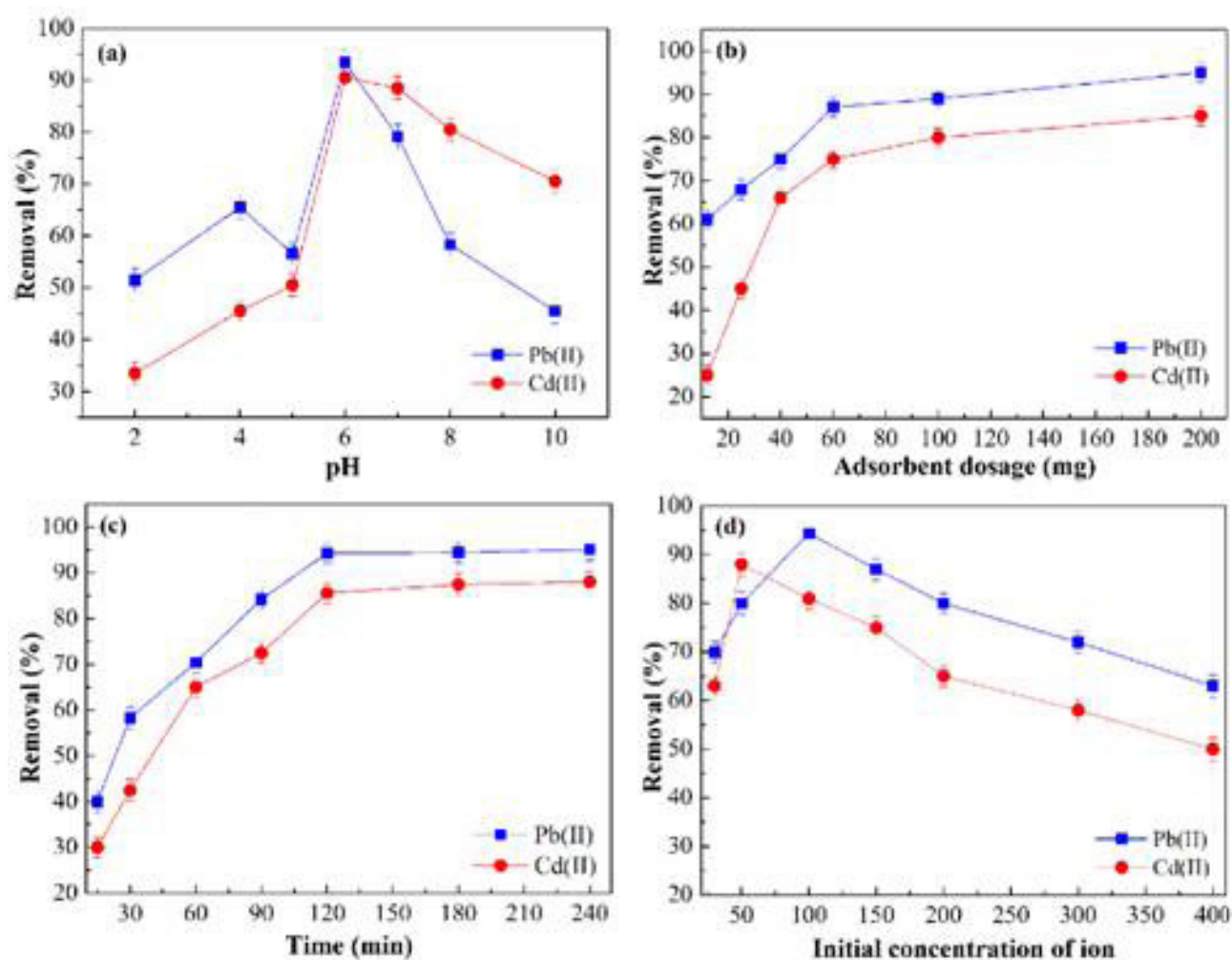


Fig. 7. Effect of solution pH (2.0–8.0), T (298K), adsorbent dose (50 mg), initial concentration (50 mg/L), Time (180), (a), adsorbent dose (12–200 mg), pH(6), T (298 K), Time (180), initial concentration (50 mg/L) (b), agitation time (20–240 min), pH (6), adsorbent dose (150 mg), T (298 K), initial concentration (50 mg/L) (c), and initial concentration of Pb(II) and Cd(II) ions (30–400 mg/L), adsorbent dose (150 mg), pH (6), T (298 K), Time (120) (d).

backbone together with the eggshell and Fe_3O_4 nano particles may result in the formation of metal ions complexes through chelation or metal exchange in the adsorbent.

3.2.2. Effect of the adsorbent dosage

Adsorbent dosage study is an essential factor in adsorption studies because it controls the capacity of adsorbent for a certain initial concentration of metal ion solution. The effect of adsorbent dosage on the percentage removal of Pb (II) and Cd (II) in the range 12–200 mg/L is shown in Fig. 7b. From Fig. 7b it can be observed that increasing the adsorbent increased the percentage removal of Pb (II) from 61.2% up to 95.0% with the required optimum dosage of 150 mg/L, while the percentage removal of Cd (II) increased from 25.2% up to 87.0% with the required optimum dosage of 150 mg/L. As can be seen in Fig. 7b, beyond the optimum dose (150 mg/L) the percentage removal did not change with the nano adsorbent dose. As expected, the percentage removal increased with increasing the nano adsorbent dose. This increase in adsorption can be due to the presence of more binding sites on the surface of the adsorbent to form complexes with Pb (II) and Cd (II) [35]. On the other hand, the decrease in percentage removal with increase in the nano adsorbent dose is mainly due to the un saturation of the adsorption sites through the adsorption process [35].

3.2.3. Effect of agitation time

The agitation time at which the adsorption takes place is one of the effective parameter in batch adsorption experiments. Therefore, it is important to find the time dependence of such systems under different process conditions. The experimental runs determining the effect of agitation time on the batch adsorption of metal ion solution containing 100 mg/L of Pb (II) and Cd (II) at 25°C, initial pH value 6, and adsorbent dose of 150 mg in 50 mL are shown in Fig. 7c. As seen from Fig. 6c, the adsorption rate for Pb (II) and Cd(II) reaches up to 95.0% and 88.0%, respectively when the contact time was 120 min, and then a slight change in the sorption rate was observed. This result indicates that the percentage removal of Pb (II) is faster than that of the Cd (II) at the contact time 120 min.

3.2.4. Effect of initial concentration

The effect of initial concentration of metal ions on the percentage removal was investigated at different concentrations (30–400 mg/L), keeping all other factors constant (Fig. 7d). The percentage removal of Pb (II) and Cd (II) ions by nano adsorbent was found to decrease with increase in Pb (II) (up to 100 mg/L) and Cd (II) (up to 50 mg/L) initial concentration. The decrease in adsorption can be ascribed to the increase in the amount of Pb (II) and Cd (II) ions while the number of available active sites on the nano adsorbent are fixed.

3.3. Desorption and regeneration studies

The adsorption results, as shown in Fig. 8, showed that the nano composite did not remove Pb (II) and Cd (II) at high acidic conditions (pH < 2), indicating that such pH val-

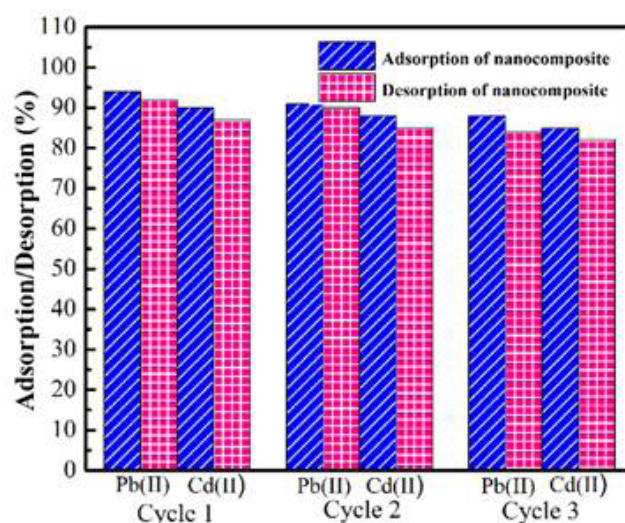


Fig. 8. Adsorption/desorption percentages of Pb (II) and Cd (II) metal ions during 3 cycles.

ues are suitable for the desorption studies. Thus, the reusability of the nano composite was examined by using HCl (0.1 M) at room temperature and the amount of Pb (II) and Cd(II) ions, desorbed in 1 h, was determined by AAS. Fig. 8 shows the percentage removal and desorption of nano composite after three cycles. The results showed that adsorption decreased only ~8% after three cycles desorption in HCl (0.1 M) solution. These results show that even three desorption steps in 0.1 M HCl did not drastically decrease the complexing ability of the nano composite. Consequently, it can be concluded that nano composite beads can be used repeatedly with a slight decrease in their adsorption capacity for the representative Pb (II) and Cd (II) metal ions.

3.4. Isotherm studies

In the current research, the adsorption isotherms were studied by using Langmuir and Freundlich, and the results are shown in Fig. 9. The Langmuir model is often applied to define the equilibrium adsorption isotherms of homogeneous surfaces and it is used successfully in mono molecular adsorption processes, whereas Freundlich model describes sorption on reversible heterogeneous surfaces [36]. Eqs. (3) and (4) represent the mathematical terms of the Langmuir and Freundlich isotherm models, respectively [35]:

$$\frac{C_e}{Q_e} = \frac{1}{Q_m K_L} + \frac{C_e}{Q_m} \quad (3)$$

$$\log Q_e = \log K_f + \frac{1}{n} \log C_e \quad (4)$$

where Q_e and Q_{max} are the equilibrium adsorption capacity (mg/g) and the maximum metal ion uptake capacity (mg/g), respectively. C_e (mg/L) is metal ion concentration at equilibrium. K_L (Lmg^{-1}) and K_f (Lmg^{-1}) are the Langmuir and Freundlich constants, respectively and are determined from the plot $\ln Q_e$ versus $\ln C_e$ and the plot C_e/Q_e vs. C_e

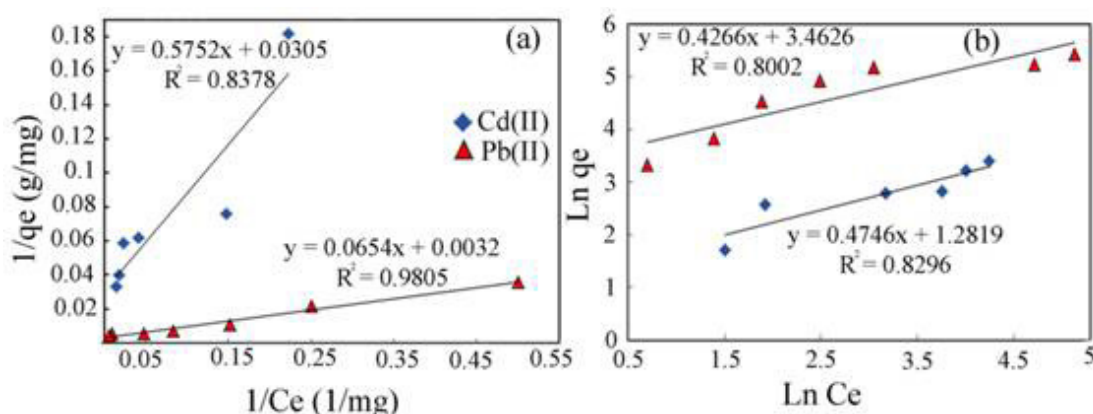


Fig. 9. The Langmuir (a) and Freundlich (b) models of nano composite for Pb(II) and Cd(II) (Conditions: initial concentration of metal ions: 30–400 mg/L, nano adsorbent dose: 150 mg, initial pH: 6, temperature: 298 K, and agitation time: 120 min).

Table 1
Isotherm model parameters and correlation coefficients for Pb (II) and Cd (II) ions

Ions	Langmuir model			Freundlich model		
	Q_m (mg g^{-1})	K_L (L mg^{-1})	R^2	K_F (mg g^{-1})	n	R^2
Pb (II)	312.5	0.0489	0.980	31.89	0.426	0.80
Cd (II)	32.78	0.053	0.837	3.60	0.474	0.82

Table 2
Comparison of the adsorption capacities of various adsorbents for Pb (II) and Cd (II) adsorption

Adsorbent	Q (mg/g)		Ref.
	Cd(II)	Pb(II)	
Magnetic chitosan grafted thiacalix[4]arene	–	23.25	[16]
Polythiophene/Sb ₂ O ₃ nanocomposite	–	18.94	[37]
Rice Straw/Fe ₃ O ₄ nanocomposite	–	19.45	[38]
Bentonite	–	52.31	[39]
Sawdust	4.39	6.54	[40]
Sporopollenin	6.72	–	[41]
Fenton activated	–	13.27	[42]
Perlite	–	8.90	[43]
Dolomite	–	18.55	[44]
M. rouxii biomass	4.00	4.00	[44]
Petiolar felt-sheath palm	11.00	11.00	[45]
Red Mud	10.57	–	[46]
Active carbon	11.27	–	[47]
Kaolin	3.04	–	[47]
Bentonite	9.27	–	[47]
Diatomite	3.24	–	[47]
Compost	9.34	–	[47]
Cellulose pulp waste	5.82	–	[47]
Bioanocomposite	32.78	312.5	Present work

respectively. $1/n$ is the intensity of the adsorption. The adsorption isotherm parameters are shown in Fig. 9 and summarized in Table 1. According to the obtained results (Table 1), the correlation coefficient (R^2) for the Pb (II) and Cd (II) ions were 0.98 and 0.83, respectively. The experimental data are more in agreement with the Langmuir isotherm than the Freundlich isotherm, indicating that the sorption process involves coverage of multi molecular layers.

The obtained maximum adsorption capacity (Q_m) parameter results of the nano adsorbent compared with some other adsorbents found in the literature are summarized in Table 2. Our nano adsorbent has high Q_m in comparison with some previously reported nano adsorbents, demonstrating that the composite nano adsorbent is a better candidate for the applications related to water treatment.

3.5. Kinetic studies

The adsorption kinetics signifies the adsorption efficiency of the adsorbents, and therefore, can define the potential applications of adsorbents. The experiments were studied in the time range of 15–240 min at room temperature using 150 mg of adsorbent for 50 mL of Pb (II) and Cd (II) ions solution (100 mg/L). To study the adsorption rate of Pb (II) and Cd (II) ions onto the adsorbent, the pseudo-first-order equation of Lagergren [Eq. (5)] and the pseudo-second-order. Eq. (6) was calculated based on the experimental data [48].

$$\log(Q_e + Q_t) = \log Q_e - \frac{k_1}{2.303} t \quad (5)$$

$$\frac{t}{Q_t} = \frac{1}{k_2 Q_e^2} + \frac{1}{Q_e} t \quad (6)$$

where k_1 (min^{-1}) and k_2 ($\text{g mg}^{-1}\text{min}^{-1}$) are the rate constant of the Lagergren and pseudo-second-order, respectively. Q_t is the amounts of metal ions sorbed at time t (mg g^{-1}); kinetic plots and parameters of two models were calculated and are given in Fig. 10 and Table 3. Obviously, it can be seen from Fig. 10 and Table 3 that the pseudo-second-order kinetic model provided a good correlation for the adsorption of Pb(II) and Cd(II) onto nano adsorbent compared to the pseudo-first-order model. Thus, the proposed mechanism for

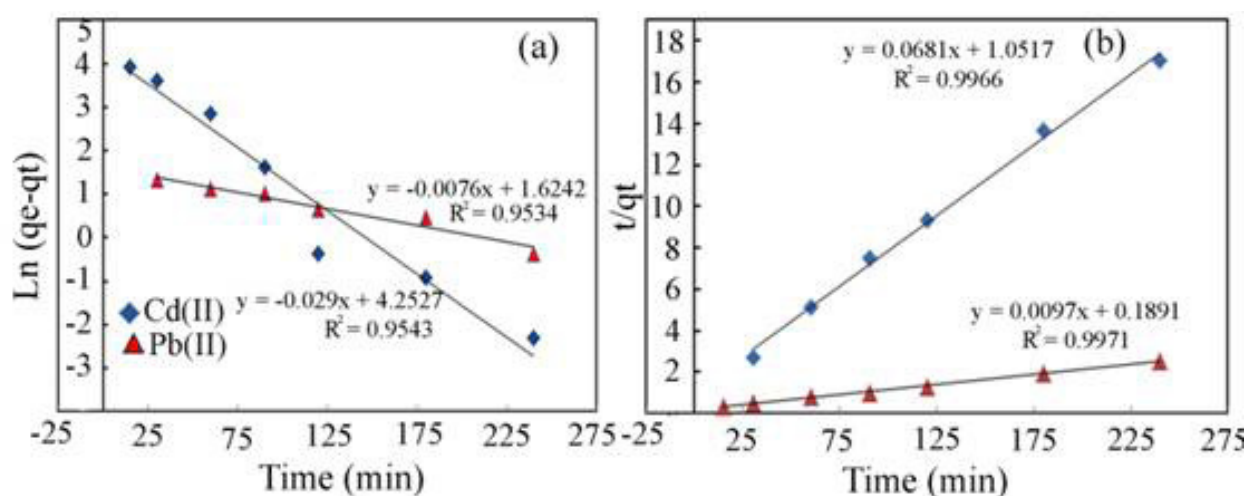


Fig. 10. The first-order (a) and second-order (b) kinetics models of nano composite for Pb (II) and Cd (II) (Conditions: initial concentration of metal ions: 100 mg/L, nano adsorbent dose: 150 mg, initial pH: 6, temperature: 298 K, and agitation time: 30–240 min).

Table 3
Kinetic models and their statistical parameters for Pb (II) and Cd (II) ions

Ions	Pseudo first order				Pseudo second order		
	$Q_{e,exp}$ (mg g ⁻¹)	k_1 (min ⁻¹)	$Q_{e,cal}$ (mg g ⁻¹)	R^2	k_2 (min ⁻¹)	$Q_{e,cal}$ (mg g ⁻¹)	R^2
Pb(II)	94.0	0.029	70.29	0.95	0.0004	103.09	0.99
Cd(II)	14.1	0.007	5.074	0.95	0.004	14.6	0.99

Table 4
Thermodynamic parameters of Pb (II) (Cd (II)) adsorption by nano composite

Temperature(K)	ΔG° (kJ/mol)	ΔH° (kJ/mol)	ΔS° (kJ/mol K)
273	-0.09(-0.45)	-	-
298	-6.56(-1.64)	-	-
303	-6.84(-2.40)	-	-
323	-7.63(-2.98)	43.38 (13.82)	0.162 (0.052)

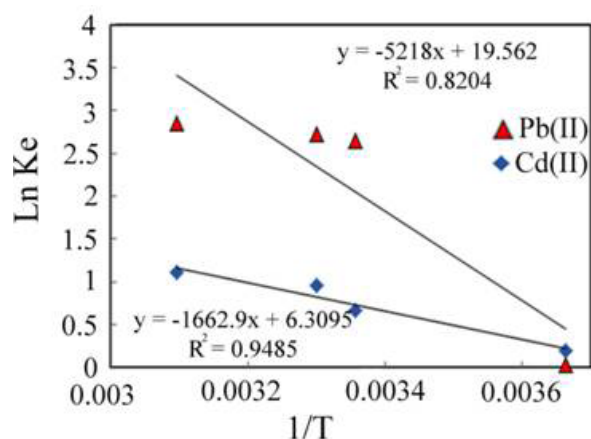


Fig. 11. Van't Hoff plots of Pb (II) and Cd (II) ions adsorption (Conditions: initial concentration of metal ions: 100 mg/L, nano adsorbent dose: 150 mg, initial pH: 6, temperature: 273–323 K, and agitation time: 120 min).

adsorption process may be controlled by physical adsorption by complex between the adsorbate and adsorbent.

Thermodynamic studies: The thermodynamic parameters such as change in enthalpy (ΔH°), change in entropy (ΔS°), and change in Gibbs free energy (ΔG°) of Pb (II) and Cd (II) adsorption onto nano composite can be associated to

the distribution coefficient of solute between the solid and liquid phases by the following equations [49]:

$$K_d = \frac{q_e}{c_e} \quad (7)$$

$$\Delta G^\circ = -RT \ln K_d \quad (8)$$

$$\ln K_d = \left(\frac{\Delta S^\circ}{R} \right) - \left(\frac{\Delta H^\circ}{RT} \right) \quad (9)$$

where K_d is the distribution coefficient. R and T are the universal gas constant (8.314 J/mol K) and absolute temperature (K), respectively. The values of ΔH° and ΔS° were achieved from the slope and intercept of the linear plot of $\ln K_d$ vs. $1/T$ as shown in Fig. 11. The thermodynamic parameters for the adsorption of Pb (II) and Cd (II) in aqueous solutions onto nano composite are summarized at various temperatures in Table 4. Values of ΔG° for Pb (II) and Cd (II) are negative, verifying that the adsorption of Pb (II) and Cd (II) ions on treated adsorbent is a spontaneous and thermodynamically favorable process. The more negative values of ΔG° suggest a greater driving force to the adsorption process. The positive values of ΔH° reveal an endothermic adsorption process, which is supported by the increase in adsorption with increasing temperature. The ΔH° magnitude offers evidence about the type of adsorption. The positive ΔS° values suggest high affinity of the sorbent for the sorbate, and increased randomness at the solid/liquid interface.

4. Conclusions

Novel eco-friendly CPNVPMA@ eggshell/Fe₃O₄ nanocomposite was introduced for the Pb (II) and Cd (II) uptake from aqueous solutions. The novel eco-friendly nano composite was characterized by FTIR, XRD, SEM, AFM and VSM. Moreover, the ability of nano composite to bind Pb (II) and Cd (II) was examined using equilibrium, kinetic and thermodynamic aspects. The equilibrium data for Pb (II) and Cd (II) were well fitted by the Langmuir model. The pseudo-second-order rate model exactly described the kinetics of adsorption of Pb (II) and Cd (II). Furthermore, the negative ΔG° values verified the spontaneous nature of the adsorption process for both Pb (II) and Cd (II). The positive ΔH° and ΔS° values presented the endothermic nature and reversibility of the adsorption of Pb (II) and Cd (II) ions. The results exhibited the possibility of CPNVPMA@ eggshell/Fe₃O₄ nanocomposite to be used as an effective adsorbent for the removal of Pb (II) and Cd (II) from aqueous solutions. This nano composite can be a suitable alternative for the most costly used adsorbents.

References

- [1] E.N. Zare, A. Motahari, M. Sillanpää, Nano adsorbents based on conducting polymer nano composites with main focus on polyaniline and its derivatives for removal of heavy metal ions/dyes: A review, *Environ Res.*, 162 (2018) 173–195.
- [2] P.B. Tchounwou, C.G. Yedjou, A.K. Patlolla, D.J. Sutton, Heavy metal toxicity and the environment, *Molec. Clin. Environ. Toxicol.*, 101 (2012) 133–164.
- [3] M. Jaishankar, T. Tseten, N. Anbalagan, B.B. Mathew, K.N. Beeregowda, Toxicity, mechanism and health effects of some heavy metals, *Interdiscip. Toxicol.*, 7 (2014) 60–72.
- [4] M.A. Barakat, New trends in removing heavy metals from industrial wastewater, *Arab. J. Chem.*, 4 (2011) 361–377.
- [5] M. Gifford, K. Hristovski, P. Westerhoff, Ranking traditional and nano-enabled sorbents for simultaneous removal of arsenic and chromium from simulated groundwater, *Sci. Total Environ.*, 601–602 (2017) 1008–1014.
- [6] R. Das, C.D. Vecitis, A. Schulze, B. Cao, A.F. Ismail, X. Lu, J. Chen, S. Ramakrishna, Recent advances in nano materials for water protection and monitoring, *Chem. Soc. Rev.*, 46 (22) (2017) 6946–7020.
- [7] R.M. Ashour, R. El-sayed, A.F. Abdel-Magied, A.A. Abdelkhalek, M.M. Ali, K. Forsberg, A. Uheida, M. Muhammed, J. Dutta, Selective separation of rare earth ions from aqueous solution using functionalized magnetite nano particles: kinetic and thermodynamic studies, *Chem. Eng. J.*, 327 (2017) 286–296.
- [8] L. Khezami, K.K. Taha, M. OuldM-hamed, O.M. Lemine, (x) ZnO(1-x)Fe₃O₄ nano crystallines for the removal of cadmium (II) and nickel (II) from water: kinetic and adsorption studies, *J. Water. Supply. Res. T.*, 66(6) (2017) 381–391.
- [9] A. Mohammadi, S. Nemati, M. Mosafieri, A. Abdollahnejhad, M. Almasian, A. Sheikhmohammadi, Predicting the capability of carboxymethyl cellulose-stabilized iron nano particles for the remediation of arsenite from water using the response surface methodology (RSM) model: Modeling and optimization, *J. Contam. Hydrol.*, 203 (2017) 85–92.
- [10] Y. Hang, H. Yin, Y. Ji, Y. Liu, Z. Lu, A. Wang, L. Shen, H. Yin, Adsorption performances of naked and 3-aminopropyl triethoxysilane-modified mesoporous TiO₂ hollow nano spheres for Cu²⁺, Cd²⁺, Pb²⁺, and Cr (VI) ions, *J. Nanosci. Nano Technol.*, 17(8) (2017) 5539–5549.
- [11] Y. Hang, H. Yin, A. Wang, L. Shen, Y. Feng, R. Liu, Preparation of titanate whiskers starting from metatitanic acid and their adsorption performances for Cu (II), Pb (II), and Cr (III) ions, *Water Air Soil Pollut.*, 225 (2014) 2095.
- [12] F. Fu, Q. Wang, Removal of heavy metal ions from waste waters: a review, *J. Environ. Manage.*, 92(3) (2011) 407–418.
- [13] E.N. Zare, M.M. Lakouraj, A. Ramezani, Effective adsorption of heavy metal cations by super-paramagnetic poly(aniline-co-m-phenylenediamine)/Fe₃O₄ nano composite, *Adv. Polym. Technol.*, 34(3) (2015) 21501 (1 of 11).
- [14] E.N. Zare, M.M. Lakouraj, A. Ramezani, Efficient sorption of Pb (II) from an aqueous solution using a poly(aniline-co-3-aminobenzoic acid)-based magnetic core-shell nano composite, *New J. Chem.*, 40(3) (2016) 2521–2529.
- [15] M.M. Lakouraj, F. Mojerlou, E.N. Zare, Nanogel and super paramagnetic nano composite based on sodium alginate for sorption of heavy metal ions, *Carbohydr. Polym.*, 106 (2014) 34–41.
- [16] M.M. Lakouraj, F. Hasanzadeh, E.N. Zare, Nanogel and super-paramagnetic nano composite of thiacalix [4] arene functionalized chitosan: Synthesis, characterization and heavy metal sorption, Iran. *Polym. J.*, 23 (2014) 933–945.
- [17] R. Hasanzadeh, P.N. Moghadam, N. Bahri-Laleh, E.N. Zare, Sulfonated magnetic nano composite based on reactive PGMA-MAn copolymer@Fe₃O₄ nano particles: effective removal of Cu (II) ions from aqueous solutions, *Int. J. Polym. Sci.*, 2016 (2016) 1–11.
- [18] P.N. Moghadam, E.N. Zareh, Synthesis of conductive nano composites based on polyaniline/poly (styrene-alt-maleic anhydride)/polystyrene, *e-Polymers*, 10 (2010) 588–596.
- [19] E.N. Zareh, P.N. Moghadam, Synthesis and characterization of conductive nano blends based on poly (aniline-co-3-aminobenzoic acid) in the presence of poly (styrene-alt-maleic acid), *J. Appl. Polym. Sci.*, 122 (2011) 97–104.
- [20] M. Baghayeri, E.N. Zare, M. Namadchian, Direct electro chemistry and electro catalysis of hemoglobin immobilized on biocompatible poly(styrene-alternative-maleic acid)/functionalized multi-wall carbon nanotubes blends, *Sensors Actuators B Chem.*, 188 (2013) 227–234.
- [21] P.N. Moghadam, E. Azaryan, B. Zeynizade, Investigation of poly(styrene-alt-maleic anhydride) copolymer for controlled drug delivery of ceftriaxone antibiotic, *J. Macromol. Sci. Part A. Pure Appl. Chem.*, 47 (2010) 839–848.
- [22] P. Hemalatha, M.K. Veeraiyah, S. Prasannakumar, K.V. Anasuya, Synthesis, characterisation and antibacterial activity of copolymer (N-vinylpyrrolidone-maleic anhydride) with N-diethylethanolamine, *Int. Res. Eng. Technol.*, 3(3) (2014) 56–64.
- [23] M. Ahmaruzzaman, V.K. Gupta, Rice husk and its ash as low-cost adsorbents in water and wastewater treatment, *Ind. Eng. Chem. Res.*, 50 (2011) 13589–13613.
- [24] C.S. Ferreira, P.L. Santos, J.A. Bonacin, R.R. Passos, L.A. Pocrifka, Rice husk reuse in the preparation of SnO₂/SiO₂ nano composite, *Mater. Res.*, 18 (2015) 639–643.
- [25] T. Chen, Y. Xiong, Y. Qin, H. Yang, P. Zhang, F. Ye, Facile synthesis of low-cost biomass-based γ -Fe₂O₃/C for efficient adsorption and catalytic degradation of methylene blue in aqueous solution, *RSC Adv.*, 7 (2017) 336–343.
- [26] A. Guijarro-Aldaco, V. Hernández-Montoya, A. Bonilla-Petriciolet, M.A. Montes-Morán, D.I. Mendoza-Castillo, Improving the adsorption of heavy metals from water using commercial carbons modified with egg shell wastes, *Ind. Eng. Chem. Res.*, 50 (2011) 9354–9362.
- [27] R. Rohim, R. Ahmad, N. Ibrahim, N. Hamidin, C.Z.A. Abidin, Characterization of calcium oxide catalyst from eggshell waste, *Adv. Environ. Biol.*, 8 (2014) 35–38.
- [28] D. Liao, W. Zheng, X. Li, Q. Yang, X. Yue, L. Guo, G. Zeng, Removal of lead (II) from aqueous solutions using carbonate hydroxyapatite extracted from eggshell waste, *J. Hazard. Mater.*, 177 (2010) 126–130.
- [29] N.A.B. Rohaizar, N.B.A. Hadi, W.C. Sien, Removal of Cu (II) from water by adsorption on chicken eggshell, *Int. J. Eng. Technol.*, 13 (2013) 40–45.
- [30] J. Zhu, S. Wei, M. Chen, H. Gu, S.B. Rapole, S. Pallavkar, T.C. Ho, J. Hopper, Z. Guo, Magnetic nano composites for environmental remediation, *Adv. Powder Technol.*, 24 (2013) 459–467.
- [31] S. Hosseini, F.E. Babadi, S.M. Soltani, M.K. Aroua, S. Babamohammadi, A.M. Moghadam, Carbon dioxide adsorption on nitrogen-enriched gel beads from calcined eggshell/sodium alginate natural composite, *Process Saf. Environ. Prot.*, 109 (2017) 387–399.

- [32] E.N. Zare, M.M. Lakouraj, M. Baghayeri, Electro-magnetic polyfuran/ Fe_3O_4 nano composite: Synthesis, characterization, antioxidant activity and its application as a biosensor, *Int. J. Polym. Mater. Polym. Biomater.*, 64 (2015) 175–183.
- [33] D. Chen, X. Xiao, K. Yang, Removal of phosphate and hexavalent chromium from aqueous solutions by engineered waste eggshell, *RSC Adv.*, 6 (2016) 35332–35339.
- [34] A.A. Farghali, M. Bahgat, A.E. Allah, M.H. Khedr, Adsorption of Pb (II) ions from aqueous solutions using copper oxide nano structures, *Beni-Suef Univ. J. Basic Appl. Sci.*, 2 (2013) 61–71.
- [35] İ. Sargin, M. Kaya, G. Arslan, T. Baran, T. Ceter, Preparation and characterisation of biodegradable pollen–chitosan micro capsules and its application in heavy metal removal, *Biore-sour. Technol.*, 177 (2015) 1–7.
- [36] Y.-M. Hao, C. Man, Z.-B. Hu, Effective removal of Cu (II) ions from aqueous solution by amino-functionalized magnetic nano particles, *J. Hazard. Mater.*, 184 (2010) 392–399.
- [37] R. Khalili, F. Shabanpour, H. Eisazadeh, Synthesis of polythio-phene/ Sb_2O_3 nanocomposite using sodium dodecylbenzene-sulfonate for the removal of Pb (II), *Adv. Polym. Technol.*, 33 (2014) 21389–21396.
- [38] R. Khandanlou, M.B. Ahmad, H.R.F. Masoumi, K. Shamel, M. Basri, K. Kalantari, Rapid adsorption of copper (II) and lead (II) by rice straw/ Fe_3O_4 nano composite: optimization, equilibrium isotherms, and adsorption kinetics study, *PLoS One*, 10 (2015) e0120264.
- [39] H.R. Rafiei, M. Shirvani, O.A. Ogunseitan, Removal of lead from aqueous solutions by a poly (acrylic acid)/bentonite nano composite, *Appl. Water Sci.*, 6 (2016) 331–338.
- [40] Y. Bulut, T.E.Z. Zeki, Removal of heavy metals from aqueous solution by sawdust adsorption, *J. Environ. Sci.*, 19 (2007) 160–166.
- [41] N. Ünlü, M. Ersoz, Removal of heavy metal ions by using dithiocarbamated-sporopollenin, *Sep. Purif. Technol.*, 52 (2007) 461–469.
- [42] P. Miretzky, C. Muñoz, Enhanced metal removal from aqueous solution by Fenton activated macrophyte biomass, *Desalina-tion*, 271 (2011) 20–28.
- [43] M. Irani, M. Amjadi, M.A. Mousavian, Comparative study of lead sorption onto natural perlite, dolomite and diatomite, *Chem. Eng. J.*, 178 (2011) 317–323.
- [44] G. Yan, T. Viraraghavan, Heavy metal removal in a biosorption column by immobilized *M. rouxii* biomass, *Bioresour. Technol.*, 78 (2001) 243–249.
- [45] M. Iqbal, A. Saeed, N. Akhtar, Petiolar felt-sheath of palm: a new biosorbent for the removal of heavy metals from contaminated water, *Bioresour. Technol.*, 81 (2002) 151–153.
- [46] E. Lopez, B. Soto, M. Arias, A. Nunez, D. Rubinos, M.T. Barral, Adsorbent properties of red mud and its use for wastewater treatment, *Water Res.*, 32 (1998) 1314–1322.
- [47] M. Ulmanu, E. Marañón, Y. Fernández, L. Castrillón, I. Anger, D. Dumitriu, Removal of copper and cadmium ions from diluted aqueous solutions by low cost and waste material adsorbents, *Water, Air, Soil Pollut.*, 142 (2003) 357–373.
- [48] Y. Lin, H. Chen, K. Lin, B. Chen, C. Chiou, Application of mag-netic particles modified with amino groups to adsorb copper ions in aqueous solution, *J. Environ. Sci.*, 23 (2011) 44–50.
- [49] S. Venkateswarlu, M. Yoon, Core–shell ferromagnetic nanorod based on amine polymer composite (Fe_3O_4 @ DAPF) for fast removal of Pb (II) from aqueous solutions, *ACS Appl. Mater. Interfaces*, 7 (2015) 25362–25372.